

Solubility Increases Associated with Crystalline Drug Nanoparticles: Methodologies and Significance

Bernard Van Eerdenbrugh,^{†,‡} Jan Vermant,[§] Johan A. Martens,^{||} Ludo Froyen,[⊥]
Jan Van Humbeeck,[⊥] Guy Van den Mooter,[‡] and Patrick Augustijns^{*,‡}

Department of Industrial and Physical Pharmacy, College of Pharmacy, Purdue University, 575 Stadium Mall Drive, West Lafayette, Indiana 47907, Laboratory for Pharmaceutics and Biopharmacy, K.U. Leuven, Gasthuisberg O&N2, Herestraat 49, Box 921, 3000, Leuven, Belgium, Department of Chemical Engineering, K.U. Leuven, W. de Croylaan 46, 3001, Leuven, Belgium, Center for Surface Chemistry and Catalysis, K.U. Leuven, Kasteelpark Arenberg 23, 3001, Heverlee, Belgium, and Metallurgy and Materials Engineering Department, K.U. Leuven, Kasteelpark Arenberg 44, 3001, Leuven, Belgium

Received June 24, 2010; Revised Manuscript Received September 1, 2010; Accepted September 7, 2010

Abstract: In this manuscript, the determination of solubility of crystalline drug nanosuspensions by a range of methods is critically investigated. As the determinations of solubility were performed in the presence of the solubilizing nanosuspension stabilizer D- α -tocopherol polyethylene glycol 1000 succinate (TPGS), the potential effects of this excipient on the measurements were studied first. Solubility data of nanosuspensions of itraconazole, lovirode, phenytoin and naproxen were generated using different methodologies. Data obtained using separation-based methodologies (centrifugation, filtration and ultracentrifugation) proved to be of limited use, due to poor nanoparticle separation efficiencies and/or significant adsorption of TPGS onto the nanoparticle surfaces. Light scattering and turbidity were found to be more suitable for the determination of nanosuspension solubility. The obtained data show that, unlike earlier reports, the solubility increases due to nanosizing are small, with measured increases of only 15%. These solubility increases are in fair agreement with what would be predicted based on the Ostwald–Freundlich equation.

Keywords: Crystalline drug nanosuspensions; solubility determination; nanosuspension solubility; Ostwald–Freundlich equation; Mie scattering

Introduction

Crystalline drug nanosuspensions are nowadays considered as a viable formulation route for the oral administration of drugs having a poor dissolution rate and/or aqueous

solubility.^{1,2} These said “nanosuspensions” are composed of submicrometer-sized crystalline drug particles, dispersed in aqueous media.³ To kinetically prevent nanoparticle agglomeration, a suitable stabilizer is typically added to the formulations.⁴ Multiple advantages have been identified with this formulation tool with respect to oral drug administration,

* Corresponding author. Mailing address: K.U. Leuven, Laboratory for Pharmaceutics and Biopharmacy, Gasthuisberg O&N2, Herestraat 49, Box 921, 3000, Leuven, Belgium. Tel: +3216330301. Fax: +3216330305. E-mail: Patrick.Augustijns@pharm.kuleuven.be.

[†] Department of Industrial and Physical Pharmacy, Purdue University.

[‡] Laboratory for Pharmaceutics and Biopharmacy, K.U. Leuven.

[§] Department of Chemical Engineering, K.U. Leuven.

^{||} Center for Surface Chemistry and Catalysis, K.U. Leuven.

[⊥] Metallurgy and Materials Engineering Department, K.U. Leuven.

(1) Kesisoglou, F.; Panmai, S.; Wu, Y. Nanosizing - Oral formulation development and biopharmaceutical evaluation. *Adv. Drug Delivery Rev.* **2007**, 59, 631–644.

(2) Van Eerdenbrugh, B.; Van den Mooter, G.; Augustijns, P. Top-down production of drug nanocrystals: nanosuspension stabilization, miniaturization and transformation into solid products (mini-review). *Int. J. Pharm.* **2008**, 364, 64–75.

(3) Rabinow, B. E. Nanosuspensions in drug delivery. *Nat. Rev. Drug Discovery* **2004**, 3, 785–796.

including an increased rate and extent of absorption, increased bioavailability of the drug and reduced fed–fasted state effects.³ The most prominent feature of the nanoparticles is their large specific surface area, resulting in an increased dissolution rate. It is through this increase in dissolution rate that the nanoparticles can be expected to express the above-mentioned advantages. However, apart from the increase in dissolution rate, an increase in solubility is often associated with nanosuspensions.^{5–9} This increase of saturation solubility is typically interpreted by the Ostwald–Freundlich equation, relating the increase in solubility to the radius (curvature) of a particle:¹⁰

$$\ln \frac{C_{s,r}}{C_{s,\infty}} = \frac{2\gamma V_m}{rRT} \quad (1)$$

with $C_{s,r}$ and $C_{s,\infty}$ the solubilities of a particle of radius r and of a very large particle, respectively, γ the interfacial tension between the solid surface and the surrounding medium, V_m the molar volume of the compound, R the universal gas constant, and T the absolute temperature. Literature reports on nanosuspension solubility have been suggested to be related to particle curvature,^{11–14} with

reported effects ranging from about 20% up to several fold increases. Müller and Peters have suggested alternative possible reasons, such as the creation of high energy surfaces.¹¹ In all of the cases, no attempt was made to quantitatively compare the observed solubility increase with what could be expected based on the Ostwald–Freundlich equation. Grant and Brittain, however, suggested that the increase in solubility due to the increased particle curvature might only become significant for particles having a radius of less than about 10 nm, based on calculations made for a hypothetical drug compound.¹⁰ Furthermore, the methodologies applied for the solubility determination in the above-cited publications all relied on filtration with pore diameters in a range of 0.1–0.22 μm . For nanosuspensions, it becomes questionable to what extent a fraction of the particulates can escape the retaining action of such filters, possibly resulting in overestimated solubility values. Certainly for poorly soluble compounds, a small overestimation in absolute terms might result in an important relative overestimation of solubility. Therefore, it is not clear whether the solubility increases reported in literature should be interpreted as an actual effect of nanosizing or rather as artifacts resulting from poor separation efficiencies of the applied filters. It is important to clarify this, to fully understand the fundamental mechanism(s) of action of crystalline drug nanosuspensions. This knowledge can help to better understand when formulation as crystalline drug nanosuspensions might be considered as a useful oral formulation tool.

This work aims to investigate solubility differences that can be associated with crystalline drug nanosuspensions. Therefore, four different model compounds (itraconazole, lovirode, phenytoin, naproxen) were formulated as nanosuspensions. For nanosuspension stabilization, 25 wt % TPGS (relative to the drug weight) was used, based on previous experience with this stabilizer indicating adequate nanosuspension stabilization.⁴ In the first part of the work, the effect of TPGS on drug solubilization was investigated. Subsequently, different separation-based methodologies for solubility determination (centrifugation, filtration and ultracentrifugation) were evaluated with respect to their suitability for determining nanosuspension solubility. As these separation-based methodologies were found to yield unacceptable and/or ambiguous results, the third part of the work describes an alternative approach probing the appearance of solid nanoparticles upon subsequent nanosuspension additions. Both light scattering and turbidity were evaluated for the monitoring of the appearance of solid material. Finally, the results obtained using the latter methodologies were compared to predictions based on the Ostwald–Freundlich equation. From these data, we were able to critically evaluate the effect size has on nanosuspension solubility.

- (4) Van Eerdenbrugh, B.; Vermant, J.; Martens, J. A.; Froyen, L.; Van Humbeeck, J.; Augustijns, P.; Van den Mooter, G. A Screening Study of Surface Stabilization During the Production of Drug Nanocrystals. *J. Pharm. Sci.* **2009**, 98, 2091–2103.
- (5) Müller, R. H.; Möschwitzer, J.; Bushrab, F. N. Manufacturing of Nanoparticles by Milling and Homogenization Techniques. In *Nanoparticle Technology for Drug Delivery, Drugs and the pharmaceutical sciences*; Gupta, R. B., Kompella, U. B., Eds.; Taylor & Francis Group, LLC: New York, 2006; Vol. 159, pp 21–51.
- (6) Müller, R. H.; Böhm, B. H. L. Nanosuspensions. In *Emulsions and Nanosuspensions for the Formulation of Poorly Soluble Drugs*; Müller, R. H., Benita, S., Böhm, B. H. L., Eds.; Medpharm Scientific: Stuttgart, 1998; pp 149–174.
- (7) Müller, R. H.; Böhm, B. H. L.; Grau, M. J. Nanosuspensions: A Formulation Approach for Poorly Soluble and Poorly Bioavailable Drugs. In *Handbook of Pharmaceutical Controlled Release Technology*; Wise, D. L., Ed.; Marcel Dekker, Inc.: New York, 2000; pp 345–357.
- (8) Radtke, M. Pure Drug Nanoparticles for the Formulation of Poorly Soluble Drugs. *New Drugs* **2001**, 3, 62–68.
- (9) Kesiosoglou, F.; Panmai, S.; Wu, Y. Application of Nanoparticles in Oral Delivery of Immediate Release Formulations. *Curr. Nanosci.* **2007**, 3, 183–190.
- (10) Grant, D. J. W.; Brittain, H. G. Solubility of Pharmaceutical Solids. In *Physical Characterization of Pharmaceutical Solids, Drugs and the pharmaceutical sciences*; Brittain, H. G., Ed.; Marcel Dekker, Inc.: New York, 1995; Vol. 70, pp 321–386.
- (11) Müller, R. H.; Peters, K. Nanosuspensions for the formulation of poorly soluble drugs - I. Preparation by a size-reduction technique. *Int. J. Pharm.* **1998**, 2, 229–237.
- (12) Hecq, J.; Deleers, M.; Fanara, D.; Vranckx, H.; Amighi, K. Preparation and characterization of nanocrystals for solubility and dissolution rate enhancement of nifedipine. *Int. J. Pharm.* **2005**, 299, 167–177.
- (13) Dai, W. G.; Dong, L. C.; Song, Y. Q. Nanosizing of a drug/carrageenan complex to increase solubility and dissolution rate. *Int. J. Pharm.* **2007**, 342, 201–207.

- (14) Gao, L.; Zhang, D.; Chen, M.; Zheng, T.; Wang, S. Preparation and Characterization of an Oridonin Nanosuspension for Solubility and Dissolution Velocity Enhancement. *Drug Dev. Ind. Pharm.* **2007**, 33, 1332–1339.

Materials and Methods

Materials. D- α -Tocopherol polyethylene glycol 1000 succinate (TPGS, Eastman Chemical Company, Kingsport, TN) was a gift from the manufacturer. Loviride and itraconazole were kindly provided by Johnson & Johnson Pharmaceutical Research and Development (Beerse, Belgium). Indomethacin (Certa n.v., Braine-l'Alleud, Belgium), naproxen (Certa n.v., Braine-l'Alleud, Belgium), phenytoin (Fagron NV, Waregem, Belgium), sulfathiazole (Certa n.v., Braine-l'Alleud, Belgium), trifluoroacetic acid HPLC grade (Fisher Scientific UK Limited, Loughborough, U.K.), acetonitrile gradient grade far UV (Fisher Scientific UK Limited, Loughborough, U.K.), methylene chloride (Fisher Scientific UK Limited, Loughborough, U.K.), tetrahydrofuran (Acros Organics, Geel, Belgium), dimethyl sulfoxide (Acros Organics, Geel, Belgium), methanol 99.9% for HPLC gradient grade (Acros Organics, Geel, Belgium), potassium dihydrogen phosphate GR for analysis (Merck KGaA, Darmstadt, Germany), dipotassium hydrogen phosphate trihydrate GR for analysis (VWR International bvba/sprl, Leuven, Belgium), tetrabutyl ammonium hydrogen sulfate (TBAH, Acros Organics, Geel, Belgium), 1 M HCl (Titrimorm, VWR International, Fontenay Sous Bois, France) and yttrium stabilized zirconia beads (diameter 0.5 mm, YTZ grinding media, Tosoh Corporation Advanced Ceramics Department, Tokyo, Japan) were obtained commercially. Demineralized water was used for all experiments (Elga, maxima ultra pure water, $\geq 18\text{ M}\Omega$).

Media Milling. Nanosuspensions were prepared using wet media milling. Suspensions of 1 g of drug compound were dispersed in 5 mL of water in 10 mL vials using 250 mg of TPGS as a stabilizer (25 wt %, relative to the drug weight). Subsequently, 15 g of beads was added as a milling agent and vials were placed in self-designed nylon holders such that up to 6 vials per holder fitted into 500 mL mixing bowls.¹⁵ The four mixing bowls were then placed into the grinding stations of a planetary mill (Retsch PM 400 MA, Retsch GmbH, Haan, Germany), and milling was performed at 250 rpm. For naproxen, itraconazole and phenytoin, milling was performed for 24 h. For loviride, different sizes were obtained by milling for different periods of time (0.25, 0.5, 1, 2, 4, 8, 16, 24, 48, and 72 h). Two batches, each containing 1 g of drug, were prepared for each nanosuspension formulation. After milling, beads were separated from the nanosuspensions and both batches were pooled and diluted with water to a target concentration of 20 mg/mL (corresponding to a TPGS concentration of 5 mg/mL). To ensure a quantitative collection of both drug and stabilizer,

beads and vials were rinsed several times with portions of the water used for dilution.

Micellar Solubilization Studies of Polymorphic Pairs. The apparent solubility of the metastable polymorphs of indomethacin and sulfathiazole (the α form and form I, respectively) and the solubility of their stable counterparts (the γ form and form III, respectively) were determined in TPGS solutions. Either the polymorphs were prepared based on well-established procedures^{16,17} or the commercially obtained product was used (γ -indomethacin). The forms were confirmed by comparing data obtained by differential scanning calorimetry and X-ray powder diffraction with reported literature data.^{16,17} For the determination of the (apparent) solubility, dissolution experiments were performed at room temperature. Therefore, an excess of compound was added to a test tube containing 10 mL of 4, 5, 6, 8, or 10 mg/mL TPGS in water. Subsequently, the test tubes were rotated on a rotary mixer at 30 rpm (model 34526, Snijders Scientific, Tilburg, The Netherlands). After 0.5, 2, 4, 6, 8, and 24 h, respectively, 1 mL of sample was withdrawn and filtered through a 0.1 μm PTFE syringe filter (Whatman Inc., Clifton, NJ). The first half of the volume was discarded and the second half collected. Subsequently, the collected sample was analyzed by HPLC–UV, as described below. From the (meta)stable plateau observed in all of the dissolution curves, the (apparent) solubility was determined by calculating the average value and standard deviation of the 6, 8, and 24 h time points.

Micellar Solubilization Studies of the Unmilled Model Drug Compounds. Solubilization as a function of TPGS concentration was determined for unmilled itraconazole, loviride, phenytoin and naproxen. Therefore, an excess of solid was added to a test tube containing 10 mL of 2, 4, 5, 6, 8, or 10 mg/mL TPGS in water. Upon equilibration for at least 24 h, the content of the test tube was filtered through a 0.1 μm PTFE syringe filter (Whatman Inc., Clifton, NJ). The final 2 mL fraction was collected and further analyzed with HPLC–UV, as described below. Each experiment was performed in triplicate, and the average and standard deviations were calculated.

HPLC Assays. Sulfathiazole sample concentrations were determined on a Merck-Hitachi-Lachrom instrument (Hitachi Ltd., Tokyo, Japan) using a Merck Chromolith Performance RP18-e (100–4.6 mm) column (Merck, Darmstadt, Germany). The mobile phase consisted of 0.02% (v/v) trifluoroacetic acid in water/acetonitrile [88/12, (v/v)], and the flow rate was 1 mL/min. For analysis, 10 μL of sample was injected and detection was carried out at 280 nm. The range of the method was 100–2.5 $\mu\text{g/mL}$. All other drug compound concentrations were quantified by previously described, validated HPLC–UV assays.⁴ All samples were analyzed after dissolving and/or diluting into the validated range.

(15) Van Eerdenbrugh, B.; Stuyven, B.; Froyen, L.; Van Humbeeck, J.; Martens, J. A.; Augustijns, P.; Van den Mooter, G. Down-scaling Drug Nanosuspension Production: Processing Aspects and Physicochemical Characterization. *AAPS PharmSciTech* **2009**, *10*, 44–53.

(16) Kaneniwa, N.; Otsuka, M.; Hayashi, T. Physicochemical Characterization of Indomethacin Polymorphs and the Transformation Kinetics in Ethanol. *Chem. Pharm. Bull.* **1985**, *33*, 3447–3455.

(17) Anwar, J.; Tarling, S. E.; Barnes, P. Polymorphism of Sulfathiazole. *J. Pharm. Sci.* **1989**, *78*, 337–342.

Particle Size Measurements by Dynamic Light Scattering.

For the evaluation of the apparent particle size of nanosuspensions, dynamic light scattering was used (DLS). For itraconazole, phenytoin and naproxen, DLS was performed using a Nanophox instrument equipped with a He–Ne laser operating at 632.8 nm, in autocorrelation mode (SympaTec GmbH, Clausthal-Zellerfeld, Germany). Prior to measurement, samples were diluted with a saturated solution of the compound under investigation. Saturated solutions were prepared by filtration of a coarse drug suspension, stirred overnight, through a 0.45 μm nylon 47 mm syringe filter (Millipore Corporation, Bedford, MA). Detection was carried out at a fixed scattering angle of 90°, the sample temperature was set at 25 °C and 3 runs of 30 s were performed on each sample. From the resulting correlation curves, a second order analysis was performed to calculate the mean particle size and standard deviation. For the apparent particle size determination of the loviride nanosuspensions and the determination of the influence of solubilized loviride on the size of the TPGS micelles, a multiangle light scattering spectrometer was used (CGS-3, Malvern Instruments, Worcestershire, U.K.) equipped with a goniometer, a uniphase 22 mW He–Ne laser operating at 632.8 nm, an avalanche photodiode and detector and an ALV-5000/EPP multiangle tau correlator. Prior to the size measurement of the loviride nanosuspensions, the nanosuspensions were diluted with a saturated solution of loviride. The size of the TPGS micelles was determined at a concentration of 5 mg/mL TPGS. The temperature of the samples was controlled at 25 °C using an external bath circulation. Three runs of 10 s were performed on each sample. From the resulting correlation curves, a second order analysis was performed to calculate the mean micellar size and standard deviation. All measurements were performed in triplicate, at scattering angle of 90°.

Nanosuspension Solubility by (Ultra)centrifugation and Filtration. For the centrifugation experiments, 1 mL of nanosuspension was transferred into 1.5 mL tubes (Eppendorf Microtubes 3810X, Eppendorf AG, Hamburg, Germany). Subsequently, the tubes were centrifuged using an Eppendorf Centrifuge (model 5804 R, Eppendorf AG, Hamburg, Germany) equipped with an Eppendorf F45-30-22 rotor (Eppendorf AG, Hamburg, Germany). Centrifugation was performed at 20 °C and 20000g. The standard centrifugation time applied was 30 min. To investigate the influence of centrifugation time on separation efficiency, a loviride nanosuspension, milled for 24 h, was centrifuged for 60, 90, and 120 min. After centrifugation, 0.5 mL of supernatant was collected for solubility determination. As filtration of the concentrated nanosuspensions was not possible due to the pressure buildup, the supernatant of centrifuged samples was filtrated through a 0.1 μm PTFE filter. Prior to the actual filtration experiment, the filter was rinsed with 2 aliquots of 0.5 mL of supernatant. Subsequently, a third aliquot was filtered to perform the actual solubility determination. For the ultracentrifugation experiments, 10 mL of the nanosuspension was placed in a plastic

test tube with a push cap [tube (13 mL, 95 \times 16.8 mm, PP) and cap, Sarstedt AG&Co, Nümbrecht, Germany]. Ultracentrifugation was performed at 100000g (36.400 rpm) for 30 min at 20 °C with a Centrikon T-2060 ultracentrifuge (Kontron Instruments S.p.a., Milan, Italy) using a fixed angle rotor (TFT 70.38, Kontron Instruments S.p.a., Milan, Italy). After ultracentrifugation, 2 mL of supernatant was carefully collected. Again, the influence of a longer ultracentrifugation time was investigated for a loviride nanosuspension milled for 24 h by using 60, 90, and 120 min time points. The exact drug concentration in the nanosuspensions (that were diluted to a target concentration of 20 mg/mL drug compound) was determined, from which the TPGS concentration was derived by dividing by 4 (25 wt % of TPGS was added, relative to the drug weight). This value was used to calculate the expected solubility of the unmilled reference material at an identical TPGS concentration, using the determined micellar solubility relationships. Nanosuspension solubility values were expressed as a percentage (relative to the expected solubility of the unmilled reference), by dividing the measured nanosuspension solubility value by the calculated solubility of the unmilled compound at the same TPGS concentration. Alternatively, values were expressed as excess concentrations (relative to the expected solubility of the unmilled reference), by subtracting the calculated solubility of the unmilled compound from the measured nanosuspension solubility. All drug concentrations were quantified by HPLC–UV, as described above. Each experiment was performed in triplicate, and the average values and standard deviations were calculated.

Nanosuspension Solubility by Scattering and Turbidity Monitoring. For these experiments, the nanosuspensions were diluted to concentrations of 0.1 mg/mL (itraconazole, loviride), 0.75 mg/mL (phenytoin) or 2 mg/mL (naproxen), keeping the TPGS concentration constant at 5 mg/mL by diluting with a 5 mg/mL TPGS solution. The exact concentrations of the suspensions were determined by HPLC–UV, as described above. Each concentration was determined in triplicate, and the average and standard deviation were determined and used for the calculation of the drug concentration in the samples used for further measurements. These samples were prepared by subsequent additions of known small amounts of the nanosuspension to a test tube containing 10 mL of 5 mg/mL TPGS. In between each subsequent addition of nanosuspension, the sample was gently shaken and left to equilibrate to ensure adequate time for dissolution processes to complete prior to a subsequent nanosuspension addition. Each sample concentration was prepared in triplicate. For scattering, the samples were analyzed in a 10 mm quartz cuvette using a luminescence spectrometer (PerkinElmer Instruments LLC, Shelton, CT). The excitation wavelength was 700 nm, and an excitation slit of 15 nm was used. The emission slit was set at 20 nm, and the emission detection wavelength was 700 nm. An integration time of 1 s was used. In case the intensity exceeded the instrument's limit, an attenuator (1% transmittance) was placed in the beam path. The exact attenuation ratio, defined

as the intensity measured with the attenuator divided by that without the attenuator, was determined experimentally. This ratio was then used to correct the intensities of attenuated measurements. After placement of a sample in the instrument, an equilibration period up to a few minutes resulted in a stable signal. The average of three subsequent measurements was taken as the intensity value of a sample. For the turbidity measurements, 200 μL of sample was transferred into a flat transparent 96 well plate (Greiner Bio-One International AG, Frickenhausen, Germany). The plates were analyzed with a Tecan infinite 200 plate reader (Tecan Austria GmbH, Grödig/Salzburg, Austria) by measuring absorbance at 700 nm. A total of 25 reads were performed on each well. The scattering intensity or absorbance as a function of the total concentration of drug compound added, including the dissolved and undissolved species, was determined. The solubility of the compound was then derived as the intersection point of the curve fitted on samples in which all drug was dissolved and that fitted on samples also containing undissolved drug nanoparticles. Points close to the intersection point, for which it is not clear whether they belong to the soluble or insoluble regime, were not used for the fitting. Additionally, points at higher concentrations were not included in the linear fit in case they deviated from linearity. All fittings were performed on at least 4 (typically more) sample points. Each solubility determination was performed in triplicate, from which the average solubility and standard deviation was determined.

Determination of the Refractive Index of Loviride. For the determination of the real part of the refractive index of loviride, Saveyn's multiple solvent approach was used.¹⁸ Therefore, 0.05, 0.1, 0.25, 0.5 and 1% (w/v) loviride solutions were prepared in different solvents (tetrahydrofuran, methylene chloride and dimethyl sulfoxide). Refractive indexes of the solutions were determined in triplicate with an automatic digital refractometer at 20.00 °C (Atago RX-7000 α , Atago Co. Ltd., Tokyo, Japan), and the refractive index was plotted as a function of drug concentration. From these curves, the slopes were calculated (dn/dc ; all correlation coefficients were >0.995). Subsequently, the refractive indexes of the pure solvents were plotted as a function of the obtained dn/dc values and the real refractive index of loviride was determined by extrapolating the linear fit of the data (correlation coefficient >0.995) to a dn/dc value of 0 (based on the reasoning that when the refractive indexes of solvent and solute are equal, dn/dv will be zero). From this a real refractive index of 1.621 was obtained for loviride.

Scattering Predictions of the Micelles Based on Mie Theory. Scattering calculations were performed using MiePlot v4.2.03. (<http://www.philiplaven.com/mieplot.htm>), a Visual Basic interface to the BHMIE code, originally developed by Bohren and Huffman.¹⁹ Scattering intensity of randomly polarized light was determined at a scattering angle of 90°.

For the calculations, the following input values were used: 1.333 (refractive index of water), 700 nm (wavelength in vacuum), 0 (absorption/imaginary refractive index of the sphere). Values for the real refractive index and size of the micelles were used depending on the nature of the calculations. The refractive indexes of the micelles were estimated by calculating the sum of the real refractive index of pure water (1.333) and pure TPGS [1.465, based on literature values for chemically similar surfactants (Tween 80 = 1.470, sodium lauryl sulfate = 1.450, poloxamer 188 = 1.479²⁰)], multiplied by their respective volume fractions in the micelles. The volume fraction of water in the micelles was estimated to be 0.73 (8 volume parts of water for each 11 volume parts) based on literature on PEO-PPO-PEO block copolymer micelles,^{21,22} resulting in a refractive index of 1.369. This value was used as such for predictions where solely the effect of size was considered. Values for the changes in the real refractive indexes of the micelles due to loviride solubilization were calculated using a fixed water/TPGS volume ratio of 8/3 and the corresponding real refractive index of 1.369. The volume fraction of loviride as a function of the solubilized concentration was determined using the density of loviride (1.44 g/mL⁴), the density of TPGS (1.08 g/mL, estimated at 25 °C from data available at higher temperatures²³) and a refractive index for loviride of 1.621. The size of the micelles was assumed constant for these predictions (12 nm). For the scenario where the size increase was assumed to be due to larger aggregation numbers of TPGS molecules (N_{agg}), the real refractive index used was 1.369. N_{agg} was assumed to be proportional to the volume of the micelles and the concentration of the micelles proportional to $1/N_{\text{agg}}$. Therefore, the scattering intensities obtained for the different sized micelles were multiplied by the ratio of the volume of a sphere of that particular size by that of a 12 nm sphere. For the calculations where the size increase was supposed to be caused by an increase in water content (with N_{agg} assumed to be constant), the water content as a function of size was determined based on 12 nm starting micelles with a water content of 0.73. From the water content as a function of micellar size, corresponding real refractive indexes were determined, based on the real refractive indexes of water (1.333) and pure TPGS (1.465).

(18) Saveyn, H.; Mermuys, D.; Thas, O.; van der Meeuwen, P. Determination of the refractive index of water-dispersible granules for use in laser diffraction experiments. *Part. Part. Syst. Charact.* **2002**, *19*, 426–432.

(19) *Absorption and scattering of light by small particles*; Bohren, C. F., Huffman, D. R., Eds.; Wiley & Sons, Inc.: New York, 1983.

(20) Keck, C. M. Cyclosporin nanosuspensions: optimized size characterization and oral formulations. PhD Thesis. http://www.diss.fu-berlin.de/diss/receive/FUDISS_thesis_000000002344.

(21) Yang, L.; Alexandridis, P. Small-angle neutron scattering investigation of the temperature-dependent aggregation behavior of the block copolymer Pluronic L64 in aqueous solution. *Langmuir* **2000**, *16*, 8555–8561.

(22) Goldmints, I.; Yu, G.; Booth, C.; Smith, K. A.; Hatton, T. A. Structure of (deuterated PEO)-(PPO)-(deuterated PEO) block copolymer micelles as determined by small angle neutron scattering. *Langmuir* **1999**, *15*, 1651–1656.

(23) Eastman Chemical Company. Vitamine E TPGS - Applications and properties; Technical Brochure; 2005, PCI-102B.

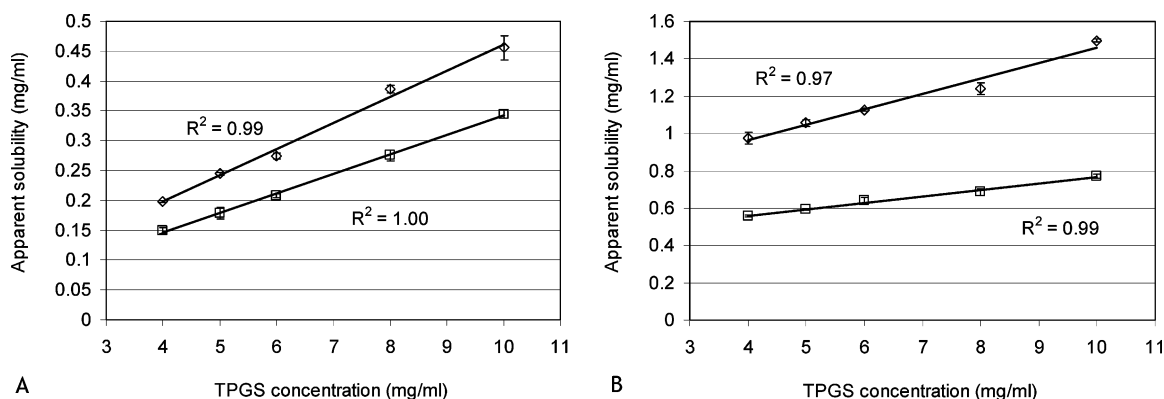


Figure 1. Micellar solubilization of different polymorphic forms as a function of TPGS concentration. Key: A = indomethacin, B = sulfathiazole, \square = stable form (γ and III, respectively), \diamond = metastable form (α and I, respectively) ($n = 3$).

Results and Discussion

Effects of Stabilizers on Solubility. In typical nanosuspension formulations, the solubility of the drug compound might be influenced by the solubilizing capacity of the stabilizers used in the formulation. Indeed, our formulations contain 25 wt % TPGS (relative to the drug weight) and TPGS is known to form micelles, with a reported CMC of 0.2 mg/mL (37 °C, phosphate buffer pH7, ionic strength 0.15 M²⁴). A key question is to what extent the higher aqueous solubility of a nanosuspension is amplified in a medium where micellar solubilization occurs. Solubility increases are the result of a higher energy state of the material due to the nanosizing process, arising from an increased particle curvature, higher energy surfaces or a less ordered structure of the material (e.g., due to partial amorphization). Will the relative increase in aqueous solubility resulting from the higher energy state of a material yield a similar relative increase in a medium where micellar solubilization occurs? To investigate this, we determined the solubilization of polymorphic pairs of indomethacin [α form (metastable) and γ form (stable), monotropic pair] and sulfathiazole [form I (metastable at room temperature) and form III (stable at room temperature), enantiotropic pair] as a function of TPGS concentration. The resulting solubilization curves are shown in Figure 1. For both compounds, the metastable form results in supersaturated systems that show a trend of higher absolute differences in drug solubilized compared to the stable form, with higher concentrations of TPGS. Furthermore, the solubility ratios, averaged for all TPGS concentrations [metastable/stable: 1.34 ± 0.04 (indomethacin), 1.81 ± 0.08 (sulfathiazole)] agree well with the reported solubility ratios of the different polymorphs in water (indomethacin, at 35 °C, 1.26;¹⁶ sulfathiazole, at 25 °C, 1.81²⁵). These data confirm that solubilities, obtained in micellar media, are indeed controlled by alterations in the energy state of the material. Furthermore, the relative increases observed are

representative for those occurring in pure water, as demonstrated by the nice agreement between the observed average solubility ratios in the presence of TPGS and the reported aqueous solubility ratios. Concluding, nanosuspension solubility in the presence of TPGS, when expressed relative to that of the unmilled reference material using identical TPGS concentrations, will be comparable to that in pure water. A second point to be made is that nanosuspensions are characterized by a very large specific surface area, typically orders of magnitude larger compared to unmilled material. Therefore a significant fraction of the stabilizer(s) can be adsorbed onto the surface of the nanosuspensions. As a result, this fraction will not be available to aid in micellar solubilization.

Nanosuspension Solubility Using Separation-Based Approaches. The standard methods used to determine drug solubility are typically separation-based techniques: centrifugation, filtration and ultracentrifugation. Hence, the suitability of these methods for nanoparticle suspension solubility determination was evaluated. To compare the obtained results with those of reference unmilled compound in the presence of equal concentrations of TPGS, micellar solubilization curves were determined for the different compounds. Results thereof are provided in Table 1. Linear fits of the apparent solubility versus TPGS concentration showed high correlation coefficients (>0.998). Furthermore, upon calculation of the solubility in a medium containing 5 mg/mL TPGS, which corresponds to the situation obtained upon diluting the suspensions to 20 mg/mL of drug compound, it can be seen that the set of compounds covers a broad solubility range (0.005–0.2 mg/mL), thereby providing a system for testing the general applicability of the methodologies evaluated. Milling times and mean particle sizes of the nanosuspensions as determined from DLS measurements are summarized in Table 2. Different mean particle sizes are obtained after 24 h of milling for the different compounds. For

(24) Yu, L.; Bridgers, A.; Polli, J.; Vickers, A.; Long, S.; Roy, A.; Winnike, R.; Coffin, M. Vitamin E-TPGS increases absorption flux of an HIV protease inhibitor by enhancing its solubility and permeability. *Pharm. Res.* **1999**, *16*, 1812–1817.

(25) Kanke, M.; Sekiguchi, K. Dissolution Behavior of Solid Drugs. II. Determination of the Transition Temperature of Sulfathiazole Polymorphs by Measuring the Initial Dissolution Rates. *Chem. Pharm. Bull.* **1973**, *21*, 878–884.

Table 1. TPGS–Solubilization Relationships, Corresponding Correlation Coefficients of the Linear Fits and Calculated Solubility in a Medium with 5 mg/mL TPGS for the Different Unmilled Compounds

compound	micellar solubilization ^a	R^2	calcd solubility in 5 mg/mL TPGS (mg/mL)
itraconazole	$y = 0.000708x + 0.001163$	>0.998	0.0047
loviride	$y = 0.00229x - 0.00064$	>0.999	0.0108
phenytoin	$y = 0.00993x + 0.0170$	>0.999	0.0667
naproxen	$y = 0.0355x + 0.0343$	>0.999	0.2116

^a With y the drug concentration (mg/ml) and x the TPGS concentration (mg/ml).

Table 2. Milling Time and Mean Particle Sizes of the Nanosuspensions Studied ($n = 3$)

compound	milling time (h)	mean particle size (nm)
itraconazole	24	220 ± 4
loviride	0.25	700 ± 88
loviride	0.5	458 ± 24
loviride	1	350 ± 14
loviride	2	301 ± 10
loviride	4	252 ± 5
loviride	8	210 ± 4
loviride	16	177 ± 4
loviride	24	162 ± 4
loviride	48	158 ± 4
loviride	72	162 ± 8
phenytoin	24	406 ± 17
naproxen	24	288 ± 4

loviride, after a gradual decrease, a plateau mean particle size of about 160 nm is reached after 24 h.

Relative solubility data for the nanosuspensions of the different compounds when milled for 24 h, as obtained using separation-based methodologies, are provided in Table 3. Figure 2 provides data for loviride nanosuspensions as a function of mean particle size (Figure 2A, centrifugation; Figure 2C, ultracentrifugation) and (ultra)centrifugation time (Figure 2B, centrifugation; Figure 2D, ultracentrifugation). Large and unrealistic increases in the relative solubility values can be noted in Table 3 for the different compounds upon solubility determination using centrifugation, an effect that becomes even more pronounced when the solubility of the unmilled compound is lower (itraconazole, loviride). In absolute terms, the excess of solubility measured clearly increases for compounds having smaller particle sizes. This trend can also be seen in the solubility values obtained for loviride as a function of particle size, depicted in Figure 2A. Although these observations could be the result of an increase in solubility, a gradual decrease in the measured solubility can be noted upon centrifugation of a loviride nanosuspension (milled for 24 h) up to 120 min (Figure 2B). This suggests that the dominating reason for the increase in measured solubility is an artifact resulting simply from poor separation of a fraction of fines. Concluding, centrifugation is not a suitable method for the determination of nanosuspension solubility. As filtration of the nanosuspensions through 0.1

μm filters was impossible due to clogging of the filters, filtration efficiency was evaluated on the supernatant of centrifuged samples. As can be seen in Table 3, trends and values obtained were similar to those obtained after centrifugation. The fact that not even a fraction of the particles can be retained by the filter suggests that filtration is even less suitable compared to centrifugation as a methodology for the characterization of the solubility of the nanosuspensions. Ultracentrifugation might be better capable of adequately separating the fine particles. Ultracentrifugation results, listed in Table 3, show lower solubility values for itraconazole and loviride compared to the unmilled situation, whereas increased solubility values were measured for phenytoin and naproxen. Results for loviride, as a function of the mean particle size of the nanosuspensions, are provided in Figure 2C. From the figure, it can be seen that a lower mean particle size results in a further lowering of the measured solubility value. This is the opposite to what would be expected based on the Ostwald–Freundlich equation, which predicts a scaling of solubility with $1/R$ (eq 1). In view of this, we have to come back to the fact that part of the TPGS will be adsorbed onto the surface of the particles which have been separated out. As a result, this fraction may not be able to participate in the micellar solubilization of the drug. In a previous study, we determined the amount of TPGS adsorbed onto the nanoparticles per square meter of surface area.⁴ The values found for the latter correspond to 6.2 ± 0.5 mg/m² (itraconazole), 4.7 ± 0.6 mg/m² (loviride), 4.5 ± 1.1 mg/m² (phenytoin) and 3.2 ± 1.2 mg/m² (naproxen). The latter values, combined with particle size data (DLS) and the density of the crystalline drugs,⁴ allow us to estimate the amount of TPGS adsorbed onto the surfaces. From this, the concentration of nonadsorbed TPGS effectively available for solubilization can be recalculated. Once this effective concentration of nonadsorbed TPGS is known, the solubility of the unmilled compound in an equal concentration of active TPGS can be estimated based on the solubilization relationships provided in Table 1. By correcting for adsorption, the solubility of the nanosuspensions can be expressed relative to that of the unmilled compound in the same concentration of nonadsorbed TPGS. It should be stressed, however, that this procedure only yields a conservative estimate rather than an exact value. As we look at the corrected values depicted in Table 3, we can see that the correction leads to more acceptable solubility values for itraconazole and loviride. The corrected data in Figure 2C even demonstrate this more clearly: smaller mean particle sizes now result in higher relative solubility values, in agreement with the trend to be expected based on the Ostwald–Freundlich equation. Finally, it is worth considering the increase in solubility obtained for phenytoin and naproxen (even prior to the adsorption correction). Both an increase in solubility and an incomplete separation efficiency of the nanoparticles might be responsible for this. Data for a loviride nanosuspension (milled for 24 h) obtained upon using longer ultracentrifugation times (Figure 2D) suggest a trend (although not significant) of lower values obtained

Table 3. Mean Particle Sizes and Obtained Solubility Data for the Nanosuspensions of the Different Compounds, Milled for 24 h^a

compound	size (nm)	solubility by centrifugation ^b (%)	excess in centrifuged supernatant ^b (mg/mL)	excess in centrifuged supernatant after filtration ^b (mg/mL)	solubility by ultracentrifugation ^b (%)	adsorption-corrected solubility by ultracentrifugation ^b (%)
itraconazole	220 ± 4	2783 ± 79	0.146 ± 0.004	0.150 ± 0.005	51.4 ± 0.3	84.7 ± 0.4
loviride	162 ± 4	2377 ± 157	0.260 ± 0.018	0.281 ± 0.019	73.3 ± 2.2	149.8 ± 4.5
phenytoin	406 ± 17	147 ± 1	0.0264 ± 0.0004	0.0267 ± 0.0007	136.1 ± 0.9	159.3 ± 1.1
naproxen	288 ± 4	136 ± 1	0.0493 ± 0.0013	0.0473 ± 0.0009	120.2 ± 0.2	139.5 ± 0.2

^a Centrifugation and ultracentrifugation were performed for 30 min. ^b Relative to the calculated solubility of the unmilled compound in a medium with equal amounts of TPGS.

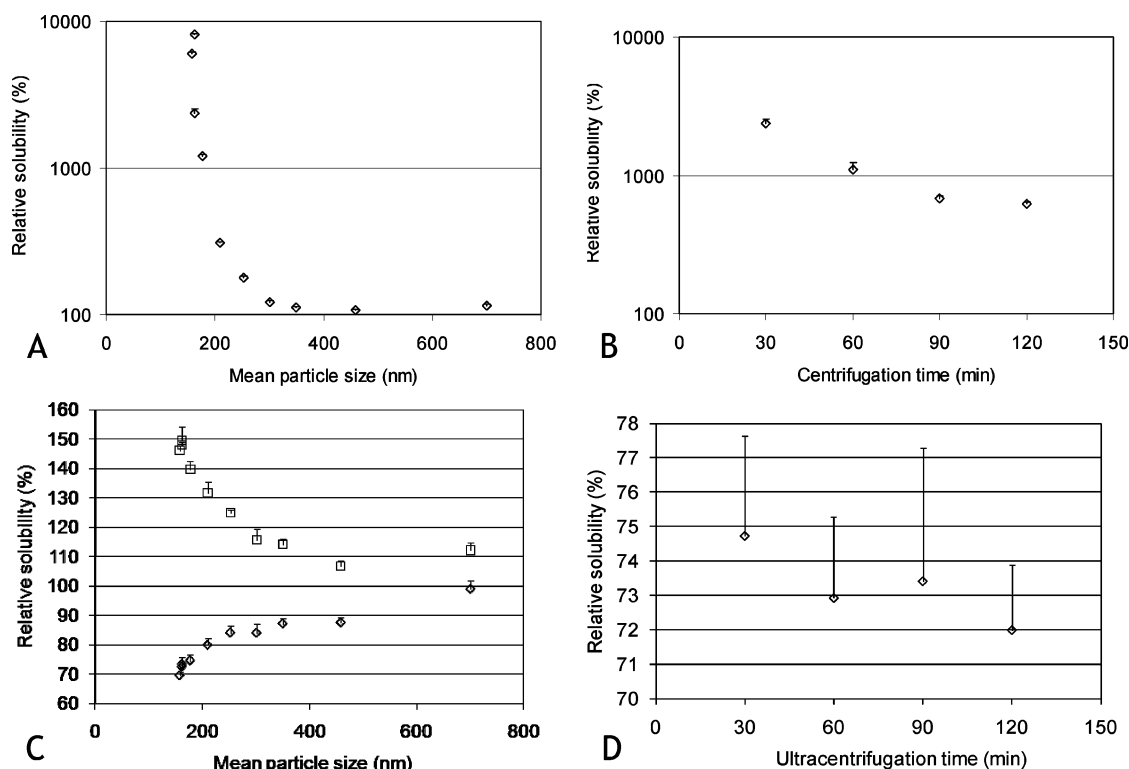


Figure 2. Solubility of loviride nanosuspensions (relative to that of the unmilled compound) as determined by centrifugation and ultracentrifugation. (A) Relative solubilities as a function of mean particle size after 30 min of centrifugation, (B) relative solubilities as a function of centrifugation time for a nanosuspension milled for 24 h, (C) relative solubilities as a function of mean particle size after 30 min of ultracentrifugation [without (\diamond) and with (\square) correction for the amount of TPGS adsorbed], and (D) relative solubilities as a function of ultracentrifugation time for a nanosuspension milled for 24 h ($n = 3$).

when using longer ultracentrifugation times. This might be due to a fraction of extremely small particles, for which even ultracentrifugation is unable to fully separate solids from dissolved material.

Concluding, all methods evaluated were shown to be unsuitable for the determination of nanosuspension solubility, due to the inability to fully separate the solubilized material from the solid nanoparticles and/or partial adsorption of TPGS onto the surfaces of the particles, thereby lowering the actual amount of TPGS available for micellar solubilization. Although the latter might be minimized by diluting the sample in media containing a fixed amount of stabilizer, hence minimizing the fraction adsorbed, the former makes it impossible to unambiguously differentiate between an increase in solubility or

poor separation efficiency. To circumvent these issues, a methodology relying on the appearance of solid material upon addition of subsequent aliquots of nanosuspension with known concentration to a medium containing a fixed concentration of TPGS (5 mg/mL) was evaluated, as described below.

Nanosuspension Solubility by Monitoring of the Appearance of Solid Material. Given the shortcomings of traditional approaches for solubility determination in the case of nanosuspensions, we evaluated a technique where the presence of undissolved nanoparticles is monitored upon subsequent nanosuspension additions. This approach was based on a previous feasibility study, showing promising yet undecisive results, where the scattering by light was moni-

tored as a function of stepwise nanosuspension additions.²⁶ This strategy of stepwise nanosuspension addition was followed to ensure that identical size distributions would be obtained for all samples with an excess of nanosuspension. For a one-step process, one could preferentially dissolve the smaller particles which would alter the particle size distribution. Since scattering is a strongly size-dependent phenomenon, this would complicate any further analysis. In the referred work,²⁶ solubility was determined from the plots of the total scattering intensity as a function of drug concentration, by extrapolation to a zero scattering intensity. The methodology was applied on amorphous nanosuspensions, using crystalline material as a reference.²⁶ For felodipine, the crystalline solubility could be determined with a relative standard deviation of about 25%, which is an encouraging result, given the very low solubility of this compound (0.8 $\mu\text{g/mL}$). In order to further develop this approach for crystalline drugs, the following adaptations were made:

(i) Since TPGS can lead to an increase of solubilized drug due to micellar solubilization, the TPGS concentration in the stock nanosuspensions and the samples prepared with the latter was kept constant at a value 5 mg/mL. Since the relative differences in solubility remain constant as a function of TPGS (see above), a higher solubility can be expected to lead to a more accurate determination of possible particle size effects on solubility.

(ii) The method proposed to determine solubility²⁶ used a linear extrapolation of the total scattering to zero intensity to infer the point of zero particle concentration. An implicit assumption here is that the scattering comes solely from the nanoparticles. When working with a medium containing a large amount of surfactant, such as 5 mg/mL of TPGS, this assumption does not hold. Scattering of the micelles will also lead to a significant contribution that cannot be ignored. Furthermore, the scattering intensity of the micelles may alter upon solubilization of a drug due to variations in size and local refractive index. This was observed in the case of loviride (Figure 3), as further discussed below. Therefore, in the present work the solubility was determined as the point of intersection of the linear fit of the region where scattering was solely due to dissolved material with the fitted curve of the region where an increase in scattering was observed due to undissolved nanoparticles.

(iii) The region where the scattered intensity is proportional to the concentration of undissolved particles is limited, as can be seen in Figure 3. This region is typically followed by a region where multiple scattering becomes important, leading to deviations from the linear scattering behavior (Figure 3). Upon using even higher concentrations, the measured scattering intensity can even start to drop. As demonstrated below, these phenomena can become problematic for compounds having higher solubility, as to limit the number of data points to be workable,

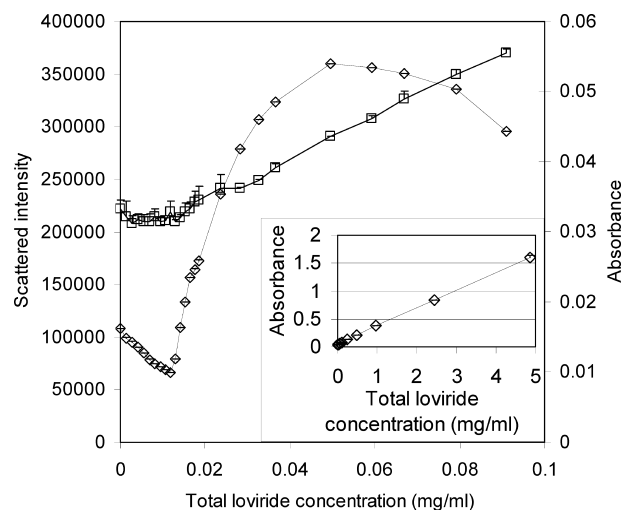


Figure 3. Scattering intensity (\diamond) and turbidity (\square) as a function of amount of drug added for a nanosuspension of loviride milled for 24 h. Inset: turbidity of the same nanosuspension in a higher concentration range ($n = 3$).

typically more nanosuspension will be added during each subsequent addition. As a result, too few data points might fall within the linear scattering range, making an unambiguous determination of the solubility difficult or even impossible. Therefore, apart from linear fits of the region of increased scattering, second order fits were also evaluated. Additionally, turbidity measurements were performed on the samples, since the response thereof was found to be linear up to much higher concentrations, as can be seen from the inset of Figure 3.

Scattering data obtained for the different compounds are shown in Figure 4. For itraconazole (Figure 4A), determination of the solubility using scattering detection resulted in a value of 0.0054 ± 0.0001 mg/mL, or $114.5 \pm 2.1\%$ of the value obtained for the unmilled suspension containing 5 mg/mL TPGS (0.0047 mg/mL). Given the weaker sensitivity of turbidity to changes in nanosuspension concentration, this technique was not precise enough to determine such a low solubility. For loviride, milled for 24 h (Figure 4B), a first remarkable observation is that the overall intensity decreases as a function of concentration in the region where no solid material is assumed to be present. This trend was also noted for the nanosuspensions that were milled for other periods of time (data not shown). It is of interest to understand why scattering tends to decrease upon micellar solubilization of loviride. As dictated by Mie theory,²⁷ the scattered intensity as a function of scattering angle of light, incident on a sphere, will depend on the wavelength of the light, the real refractive index of the sphere, the refractive index of the surrounding medium, the absorbance of the sphere and the size of the sphere. Both the incident wavelength (700 nm) and the

(26) Lindfors, L.; Forssén, S.; Skantze, P.; Skantze, U.; Zackrisson, A.; Olsson, U. Amorphous Drug Nanosuspensions. 2. Experimental Determination of Bulk Monomer Concentrations. *Langmuir* 2006, 22, 911–916.

(27) van de Hulst, H. C. Rigorous scattering theory for spheres of arbitrary size (Mie theory). In *Light Scattering by Small Particles*; van de Hulst, H. C., Ed.; Dover Publications, Inc.: New York, 1981; pp 114–130.

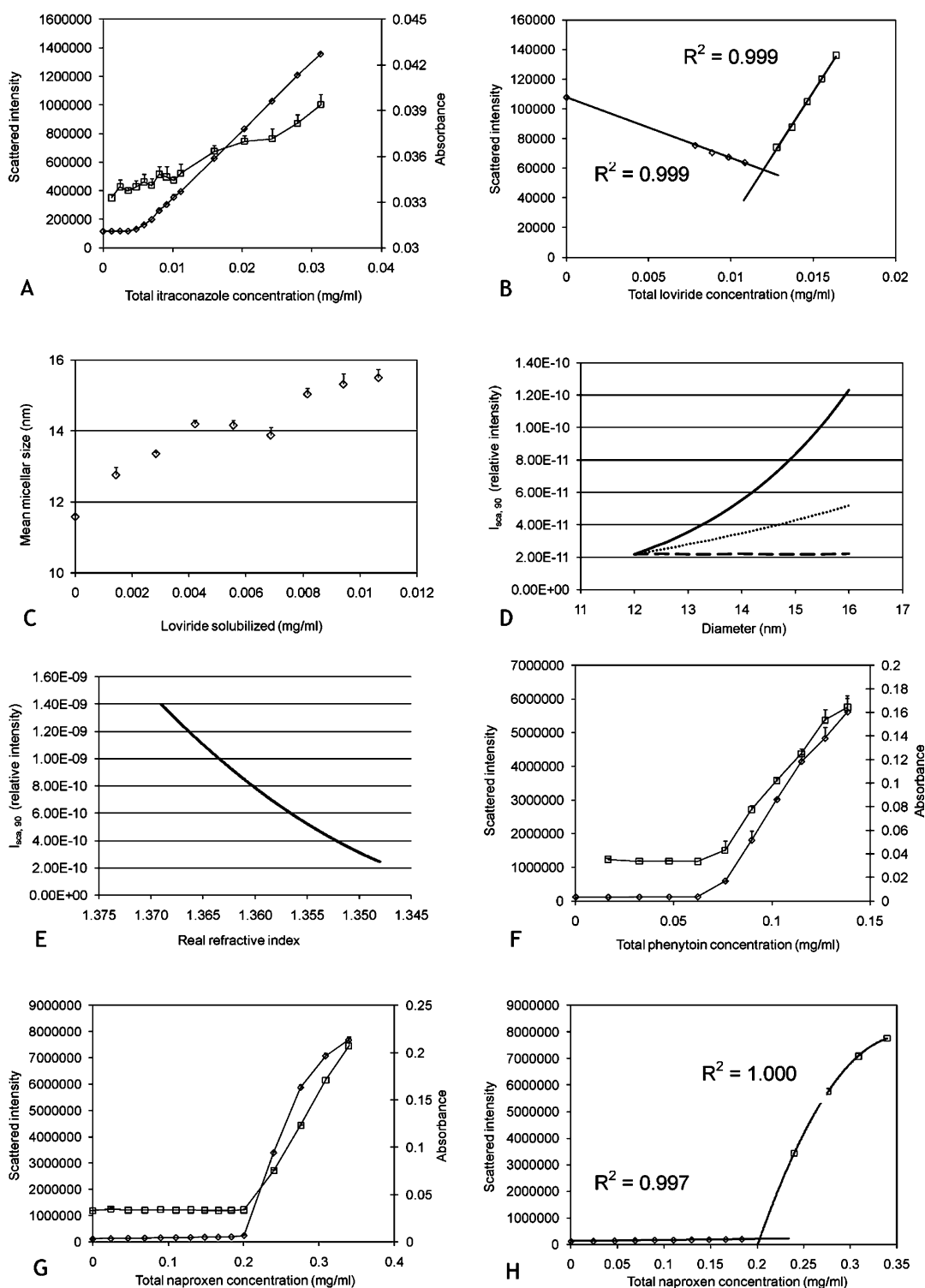


Figure 4. (A) Scattering (\diamond) and turbidity (\square) data for the itraconazole nanosuspension. (B) Linear fit of the scattering data for a loviride nanosuspension: region without (\diamond) and with (\square) undissolved nanoparticles. (C) Size of the micelles as a function of loviride added. (D) Mie calculations of scattering intensity at 90° ($I_{\text{sca},90^\circ}$) as a function of micellar size. Key: (—) using a constant real refractive index of 1.369; ($\cdot \cdot \cdot$) same as previous, applying a concentration correction to the larger sizes of $1/N_{\text{agg}}$; and (---) the increase in volume is assumed to be due to an increase in water content of the micelles. (E) Mie calculations of scattering intensity at 90° ($I_{\text{sca},90^\circ}$) of 12 nm micelles as a function of the real refractive indexes that can be expected when micellar size variations are thought to be due to changes in water content of the micelles. (F) Scattering (\diamond) and turbidity (\square) data for the phenytoin nanosuspension. (G) Scattering (\diamond) and turbidity (\square) data for the naproxen nanosuspension. (H) Second order fit of the scattering data for the naproxen nanosuspension: region without undissolved nanoparticles (\diamond , linear fit) and with undissolved nanoparticles (\square , second order fit).

refractive index of the medium (1.333) are constant during the solubilization process. The origin of the differences seen should be sought in changes in size, effective refractive index and/or aggregation number (N_{agg} , the average number of TPGS molecules present in a micelle) of the micelles. Size effects during solubilization are known to depend on the compound being solubilized.^{28,29} For loviride, size data clearly point to an increasing micellar size upon micellar solubilization, with hydrodynamic diameters of the micelles increasing from 12 to 16 nm (Figure 4C). Changes in the real refractive index considered absent, this size increase would imply an increase in scattered intensity at 90° ($I_{\text{sca},90^\circ}$, the angle at which the scattering experiments were conducted) with a factor of 5.61, as shown in Figure 4D. This clearly is in contrast with the observed decreasing trend in scattering. However, changes of the real refractive index and the aggregation number of the micelles (N_{agg} , the number of TPGS molecules per micelle) should also be evaluated, as during solubilization a number of changes in micellar composition might occur due to (i) the presence of increasing numbers of solubilized loviride molecules, (ii) differences in N_{agg} , and (iii) changes in the volume fraction of water present in the micelles. Although, in reality, all the above processes can be expected to take place simultaneously, we will evaluate them separately here, to understand their relative importance. The influence of the presence of solubilized loviride molecules on the effective refractive index of the micelles is small, leading to increases in the real refractive index of the micelles from 1.3690 (no loviride) to 1.3691 (0.012 mg/mL loviride). For a given micelle size (12 nm) the effect on $I_{\text{sca},90^\circ}$ can be expected to be negligible. Would the changes in the hydrodynamic size of the micelles be interpreted as being solely due to an increase in N_{agg} , a reduction in the concentration of scatterers (i.e., micelles) by a factor $1/N_{\text{agg}}$ would follow. This effect is illustrated in Figure 4D. Although $I_{\text{sca},90^\circ}$ is greatly reduced, scattering intensity still increases with a factor of 2.37 with increasing size. In an alternative scenario, size changes can be assumed to be caused solely by changes in the water content of the micelles (i.e., N_{agg} is supposed to be constant), hence lowering the real refractive index of the micelles from 1.369 (12 nm micelles) to 1.348 (16 nm micelles). As can be observed from Figure 4E, for 12 nm micelles, this drop in real refractive index greatly reduces $I_{\text{sca},90^\circ}$ (factor of 5.73), thereby completely neutralizing the effect of increases in scattering intensity due to larger sized micelles (Figure 4D). Concluding, we can state that solubilized loviride as such will not influence the scattered intensity to a large extent. Rather, it will have an effect on the size of the micelles. While the increase in scattering due to size is significantly reduced by the concentration effect of an increasing N_{agg} , the increase

in water content does so to a much larger extent, by lowering the refractive index, and can thus be suggested to be responsible for the observed decrease in scattering.

Solubility values obtained for loviride (Figures 3 and 4B), calculated from the scattering data, resulted in a solubility value of 0.0119 ± 0.0000 mg/mL or $110.5 \pm 0.4\%$ of the value obtained for the unmilled compound (0.0108 mg/mL). As for itraconazole, the low solubility of the compound did not allow solubility determination through turbidity data. For phenytoin (Figure 4F), it was possible to determine the solubility from both scattering (0.0711 ± 0.0007 mg/mL) and turbidity data (0.0700 ± 0.0034 mg/mL), yielding comparable values of $106.7 \pm 1.0\%$ and $105.0 \pm 5.2\%$, compared to the unmilled reference material (0.0667 mg/mL). The higher precision obtained using scattering data makes this approach better suited in this case. Finally, for naproxen (Figure 4G), it is clear that linearization of the data is only feasible for the turbidity data. The scattering data do not contain sufficient points to perform a linearization. By using a second order fit (Figure 4H), however, the latter could be successfully fitted (correlation coefficient = 1.000). Values obtained using both approaches yielded comparable solubility values of 0.2053 ± 0.0030 mg/mL (scattering) and 0.2083 ± 0.0024 mg/mL (turbidity). This corresponds to solubility values of $97.0 \pm 1.4\%$ and $98.4 \pm 1.1\%$ respectively, compared to the unmilled material (0.2116). Concluding, both scattering and overall turbidity could be successfully applied for the determination of nanosuspension solubility, which is not surprising as they reflect similar physical phenomena. However, they are complementary. Whereas scattering is the technique of choice in scenarios of low scattering intensities, turbidity may be more successful in its application when scattering intensities are higher.

Does Size Matter? As the approach evaluated in the previous section yielded results that were reproducible and close to those of the unmilled materials, we further compared them with calculations based on the increases in solubility predicted by the Ostwald–Freundlich equation. The latter equation has been applied earlier e.g. for the interpretation of observed increases of supersaturation levels of amorphous itraconazole nanoparticles.³⁰ For our calculations, a temperature of 25°C was used and the interfacial tension (γ) was estimated as described elsewhere.³¹ Here, it was shown that, using an approach based on Bragg–Williams theory, a fair estimation of the interfacial tension between solid and water could be made using the equation

$$\gamma = -\frac{0.33k_{\text{B}}T}{(V_{\text{m}}/N_{\text{A}})^{2/3}}[\ln(S_0/55.6) + 5] \quad (2)$$

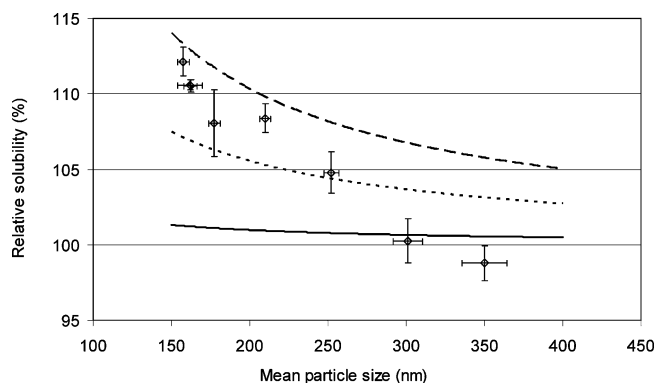
with k_{B} the Boltzmann constant, T the absolute temperature, V_{m} the molar volume of the compound, N_{A} Avogadro's number and S_0 the molar solubility of the compound in water. Furthermore, based on the interfacial tension values provided in the reference,³¹ a typical range for pharmaceuticals between 5 and 50 mN/m can be suggested. It should be stressed that the above-mentioned surface tensions are for pristine

- (28) Sharma, P. K.; Bhatia, S. R. Effect of anti-inflammatories on Pluronic® F127: micellar assembly, gelation and partitioning. *Int. J. Pharm.* **2004**, *278*, 361–377.
- (29) Sharma, P. K.; Reilly, M. J.; Jones, D. N.; Robinson, P. M.; Bhatia, S. R. The effect of pharmaceuticals on the nanoscale structure of PEO-PPO-PEO micelles. *Colloids Surf.* **2008**, *B61*, 53–60.

Table 4. Calculated Values for the Interfacial Tension, Calculated Increases in Solubility Based on the Ostwald–Freundlich Equation (for Different Interfacial Tension Values) and Measured Solubility Increases for the Different Compounds, Milled for 24 h

compound	calcd interfacial tension ^a (mN/m)	calcd rel solubility (%)			measd rel solubility (%)
		with interfacial tension of 5 mN/m	with interfacial tension as calcd	with interfacial tension of 50 mN/m	
itraconazole	20.0	102	108	121	114.5 ± 2.1 (scattering)
loviride	27.5	101	107	113	110.5 ± 0.4 (scattering)
phenytoin	24.4	100	102	104	106.7 ± 1.0 (scattering) 105.0 ± 5.2 (turbidity)
naproxen	23.6	101	102	105	97.0 ± 1.4 (scattering) 98.4 ± 1.1 (turbidity)

^a All input values used for the calculations were taken from the literature.⁴

**Figure 5.** Solubility of loviride nanosuspensions as a function of mean particle size. Key: (◇) measured values from experiments using scattering monitoring ($n = 3$), (—) calculated data using an interfacial tension of 5 mN/m, (· · ·) calculated data using the estimated interfacial tension of 27.5 mN/m, and (---) calculated data using an interfacial tension of 50 mN/m.

interfaces. In reality, TPGS molecules will be adsorbed onto the surfaces, which will lower the surface tension between solid and liquid. Hence, the values calculated for the bare surfaces will present conservative estimates. Results of the calculated relative solubility using the Ostwald–Freundlich equation are summarized in Table 4. Although the measured solubility values tend to be a little higher compared to those calculated based on surface tension estimation, both follow a similar trend. Furthermore, the values tend to lie within or at least very near to the interval covered by interfacial tension values of 5 and 50 mN/m. The same exercise was performed on the loviride nanosuspensions having different sizes, as shown in Figure 5. A clear trend in solubility increase can be noted for smaller mean particle sizes in the measured values. The data on the nanosuspensions milled for 0.25 and 0.5 h are not included here since precipitation of the nanoparticles during measurement made a proper determination of the scattering intensities impossible. Apart from the two points with mean particle sizes around 300 and 350 nm, all points fall in between the calculated curves using the calculated interfacial tension value of 27.5 mN/m or a value of 50 mN/m.

Concluding, the increases in solubility observed by light scattering and turbidity are small and in fair agreement with

what can be expected based on the Ostwald–Freundlich equation. There are some assumptions which may not be fulfilled: (i) spherical particles are supposed for the determination of the mean particle size with DLS, (ii) the interfacial tension values used in the calculations are estimates and neglect the presence of TPGS, and (iii) there are experimental errors associated with the determination of the concentrations of the stock nanosuspensions and the micellar solubilization of the unmilled materials. Yet the trends in the data are clear and suggest that, apart from this small effect originating from particle curvature, no other significant sources of solubility increase occur e.g. due to partial amorphization or the creation of higher energy surfaces. It should be mentioned that the latter might be influenced by the manufacturing process and conditions applied for nanonization. However, in the case in which nanosuspensions would be obtained having significantly higher solubility, monitoring the physical stability of the system becomes imperative, as the higher solubility combined with the high surface area available for dissolution and precipitation favors rapid kinetics of the lowering of the material's energy through a solution-mediated mechanism.³² Furthermore, the fact that the large specific surface area of nanoparticles might limit the solubilizing capacity of formulation additives due to adsorption might even lead to a lowering of the overall solubilizing capacity of the formulation. In contrast to what is often argued in the literature, we conclude that a significant increase in solubility of crystalline drug nanosuspensions should not be expected based on the increased curvature of the particles for typical sized drug nanoparticles.

Conclusions

The micellar solubilization data of different polymorphs of indomethacin and sulfathiazole confirmed that TPGS in

- (30) Matteucci, M. E.; Brettmann, B. K.; Rogers, T. L.; Elder, E. J.; Williams, R. O.; Johnston, K. P. Design of Potent Amorphous Drug Nanoparticles for Rapid Generation of Highly Supersaturated Media. *Mol. Pharmaceutics* **2007**, *4*, 782–793.
- (31) Lindfors, L.; Forssén, S.; Westergren, J.; Olsson, U. Nucleation and crystal growth in supersaturated solutions of a model drug. *J. Colloid Interface Sci.* **2008**, *325*, 404–413.
- (32) Zhang, G. G. Z.; Law, D.; Schmitt, E. A.; Qiu, Y. Phase transformation considerations during process development and manufacture of solid oral dosage forms. *Adv. Drug Delivery Rev.* **2004**, *56*, 371–390.

the medium does not significantly affect relative solubility differences between materials of a compound having different energy states. The solubility data generated using separation-based methodologies proved to be unable to yield unambiguous results, due to a poor capability in separating off all of the nanoparticles. Furthermore, the data indicated that, for nanosuspensions, a lowering of the solubilizing capacity of stabilizers can occur, due to adsorption of significant amounts of stabilizer onto the nanoparticle surfaces. Using methodologies relying on the appearance of undissolved material upon subsequent nanosuspension additions, probed by light scattering at a fixed angle and turbidity, acceptable solubility values could be generated. Whereas scattering is the technique of choice in scenarios of low scattering intensities, turbidity may be more successful in its application when scattering intensities are higher. Overall, it was found that the increases in solubility were relatively small and comparable to those calculated based on the Ostwald–Freundlich

equation. Therefore, we would like to make the following final two conclusions with respect to the solubility of crystalline drug nanosuspensions: First, a critical selection of the analytical methodology is key for the generation of valid solubility results, nonseparation based techniques being strongly preferred. Second, significant increases in solubility should not be associated with crystalline drug nanosuspensions. Rather, the rapid dissolution (and precipitation) kinetics should be regarded as the main characteristics upon evaluating the value of this formulation tool for oral drug product development.

Acknowledgment. The work was carried out within the framework of an interdisciplinary research project sponsored by K.U. Leuven (IDO-project IDO/04/009). B.V.E. is a Postdoctoral Researcher of the “Fonds voor Wetenschappelijk Onderzoek”, Flanders, Belgium.

MP100209B